Blue-Shifted and Red-Shifted Hydrogen Bonds: Theoretical Study of the $CH_3CHO\cdots HNO$ Complexes

YONG YANG, WEIJUN ZHANG, XIAOMING GAO

Laboratory of Environmental Spectroscopy, Anhui Institute of Optics and Fine Mechanics, Chinese Academy of Sciences, Hefei 230031, People's Republic of China

Received 8 August 2005; accepted 16 September 2005
Published online 14 November 2005 in Wiley InterScience (www.interscience.wiley.com).
DOI 10.1002/qua.20873

ABSTRACT: The blue-shifted and red-shifted H-bonds have been studied in complexes $CH_3CHO\cdots HNO$. At the MP2/6-31G(*d*), MP2/6-31+G(*d*,*p*) MP2/6-311++G(*d*,*p*), B3LYP/6-31G(*d*), B3LYP/6-31+G(*d*,*p*) and B3LYP/6-311++G(*d*,*p*) levels, the geometric structures and vibrational frequencies of complexes $CH_3CHO\cdots HNO$ are calculated by both standard and CP-corrected methods, respectively. Complex A exhibits simultaneously red-shifted C—H$\cdots$O and blue-shifted N—H$\cdots$O H-bonds. Complex B possesses simultaneously two blue-shifted H-bonds: C—H$\cdots$O and N—H$\cdots$O. From NBO analysis, it becomes evident that the red-shifted C—H$\cdots$O H-bond can be explained on the basis of the two opposite effects: hyperconjugation and rehybridization. The blue-shifted C—H$\cdots$O H-bond is a result of conjunct C—H bond strengthening effects of the hyperconjugation and the rehybridization due to existence of the significant electron density redistribution effect. For the blue-shifted N—H$\cdots$O H-bonds, the hyperconjugation is inhibited due to existence of the electron density redistribution effect. The large blue shift of the N—H stretching frequency is observed because the rehybridization dominates the hyperconjugation. Int J Quantum Chem 106: 1199–1207, 2006

Key words: red-shifted H-bond; blue-shifted H-bond; AIM topological analysis; NBO analysis

Correspondence to: Y. Yang; e-mail: yonyang@aiofm.ac.cn
Contract grant sponsor: National Natural Science Foundation of China.
Contract grant number: G20477043.
Contract grant sponsor: Chinese Academy of Sciences (Knowledge Creative Program).
Contract grant number: KJCX2-SW-H08.

Introduction

The unusual phenomenon of the blue-shifted X—H···Y H-bond, which is accompanied by X—H bond contraction and a blue shift of the X—H bond stretching frequency, continues to receive significant experimental and theoretical attention [1–28]. Hobza and Havlas [9] have suggested a two-step mechanism that involves electron density transfer (EDT) from the proton acceptor to the remote part of the proton donor, which in turn leads to a shortening of the X—H bond. Thus, the red-shifted and the blue-shifted H-bonds were deemed to have different origins. Having a different view, some researchers favor the view that there are no fundamental differences in the nature of red-shifted and blue-shifted H-bonds [20–28]. In addition, the blue-shifted H-bonds that have been studied so far are mainly C—H···Y systems. N—H···Y blue-shifted H-bonds are very interesting because the N atom is more electronegative than the C atom, and the N—H bond is a better proton donor than the C—H bond. Both Hobza [8] and Li et al. [24] have predicted a blue-shifted N—H···F H-bond existing in the complex NHF_2···HF at the MP2/6-31G(*d*,*p*) and MP2/6-311+G(*d*,*p*), respectively. Unexpectedly, Lu et al. [29] have predicted a red-shifted N—H···F H-bond in the complex NHF_2···HF at the B3LYP/6-31+G(*d*,*p*), B3LYP/6-311+G(*d*,*p*) and B3LYP/6-311++G(3*df*,3*pd*) levels, respectively. Both MP2 and B3LYP computations have their own supporting instances from the point of agreement between theoretical prediction and experimental measurement [2, 17]. Consequently, it is difficult to decide which H-bond type the N—H···F is from the point of theory in the NHF_2···HF complex. To the best of our knowledge, it is not yet known whether blue-shifted H-bonds can be observed in the N—H···O systems. One goal of this article is to find a case of N—H···O blue-shifted H-bond where hyperconjugative $n(O) \rightarrow \sigma^*$ (N—H) interaction is relatively strong and N—H bond has a substantial blue shift.

Acetaldehyde(CH_3CHO) is among the most abundant carbonyls in the atmosphere [30]. HNO is very important in processes such as pollution formation, energy release in propellants and fuel combustion [31, 32]. To the best of our knowledge, no investigations on the interesting red-shifted and blue-shifted H-bonds in the CH_3CHO···HNO complexes are performed up to now. In the present work, we study the H-bonds in the CH_3CHO···HNO complexes. Our next goal is expected to provide a reasonable explanation about the origins of blue-shifted and red-shifted H-bonds.

Computational Methods

STRUCTURES AND VIBRATIONAL FREQUENCIES OF THE COMPLEXES

CH_3CHO···HNO are investigated using both standard and counterpoise-corrected (CP) optimization at the MP2/6-31G(*d*), MP2/6-31+G(*d*,*p*), MP2/6-311++G(*d*,*p*), B3LYP/6-31G(*d*), B3LYP/6-31+G(*d*,*p*) and B3LYP/6-311++G(*d*,*p*) levels, respectively [33, 34]. The structures and vibrational frequencies of the monomers CH_3CHO and HNO are investigated using standard optimization at same levels. The basis set superposition errors (BSSE) are calculated according to the counterpoise method proposed by Boys and Bernardi [34]. Natural bond orbital (NBO) [35] analysis is performed at the MP2/6-31+G(*d*,*p*) level. Atoms in molecules (AIM) [36] analysis is also carried out at the MP2/6-31+G(*d*,*p*) level. All the calculations are performed using the Gaussian 03 program packages [37].

Results and Discussion

GEOMETRIES, FREQUENCIES, AND ENERGIES

The characteristics of complexes CH_3CHO···HNO determined by both standard and counterpoise-corrected (CP) optimization procedures, are presented in Tables I and II and Figure 1. From the X—H stretching frequency change between the monomers CH_3CHO and HNO and complexes CH_3CHO···HNO shown in Tables I and II, we can see that there is a slight difference between MP2 and B3LYP calculations. For example, the MP2/6-311++G(*d*,*p*) computation predicts that N8—H9 stretching frequency of the monomer HNO and complex A is 3027 and 3165 cm^{-1}, respectively, which implies 138 cm^{-1} blue shift of the N8—H9 stretching frequency. The B3LYP/6-311++G(*d*,*p*) computation predicts 142 cm^{-1} blue shift of the N8—H9 stretching frequency with that of the monomer and complex A being 2862 and 3004 cm^{-1}, respectively. As far as the H-bond type prediction is concerned, the MP2 computation re-

TABLE I

Characteristics of complexes A and B with different (standard and CP-corrected) optimization at MP2/6-31G(*d*), MP2/6-31+G(*d,p*), and MP2/6-311++G(*d,p*) levels.

		MP2/6-31G(*d*)		MP2/6-31+G(*d,p*)		MP2/6-311++G(*d,p*)	
		Standard	CP	Standard	CP	Standard	CP
A	r(O4· · ·H8) (Å)	2.1416	2.2150	2.1367	2.2116	2.1721	2.2406
	r(O10· · ·H3) (Å)	2.4558	2.6378	2.5639	2.6780	2.5994	2.7140
	Δr(N9—H8) (Å)	−0.0086	−0.0074	−0.0061	−0.0060	−0.0074	−0.0066
	$\Delta\nu$(N9—H8) (cm^{-1})	+161	+138	+126	+122	+138	+129
	Δr(C1—H3) (Å)	+0.0004	+0.0003	+0.0002	+0.0001	+0.0002	+0.0001
	$\Delta\nu$(C1—H3) (cm^{-1})	−2, −3	−2, −2	−2, −1	−1, −1	−2, −1	−1, −1
	ΔE (kcal mol^{-1})	−6.80	−6.59	−5.46	−5.39	−4.83	−4.77
	ΔE^{CP} (kcal mol^{-1})	−3.71	−3.87	−4.13	−4.21	−3.72	−3.78
	$\Delta E^{CP,ZPE}$ (kcal mol^{-1})	−1.75	−2.37	−2.71	−2.85	−2.43	−2.49
B	r(O4· · ·H8) (Å)	2.1492	2.2285	2.1526	2.2207	2.1830	2.2574
	r(O10· · ·H5) (Å)	2.5999	2.8676	2.7373	2.8527	2.7975	2.9017
	Δr(N9—H8) (Å)	−0.0091	−0.0078	−0.0062	−0.0060	−0.0069	−0.0068
	$\Delta\nu$(N9—H8) (cm^{-1})	+162	+139	+121	+118	+128	+126
	Δr(C1—H5) (Å)	−0.0059	−0.0033	−0.0036	−0.0031	−0.0035	−0.0031
	$\Delta\nu$(C1—H5) (cm^{-1})	+75	+45	+50	+45	+47	+42
	ΔE (kcal mol^{-1})	−6.27	−6.02	−5.39	−5.33	−4.72	−4.66
	ΔE^{CP} (kcal mol^{-1})	−3.42	−3.61	−4.08	−4.14	−3.60	−3.66
	$\Delta E^{CP,ZPE}$ (kcal mol^{-1})	−1.78	−2.30	−2.78	−2.86	−2.39	−2.45

TABLE II

Characteristics of complexes A and B with different (standard and CP-corrected) optimization at B3LYP/6-31G(*d*), B3LYP/6-31+G(*d,pd,p*) levels.

		B3LYP/6-31G(*d*)		B3LYP/6-31+G(*d,p*)		B3LYP/6-311++G(*d,p*)	
		Standard	CP	Standard	CP	Standard	CP
A	r(O4· · ·H8) (Å)	2.0927	2.1418	2.1160	2.1384	2.1261	2.1459
	r(O10· · ·H3) (Å)	2.4133	2.5225	2.5882	2.6000	2.6079	2.6104
	Δr(N9—H8) (Å)	−0.0107	−0.0098	−0.0070	−0.0072	−0.0079	−0.0081
	$\Delta\nu$(N9—H8) (cm^{-1})	+174	+157	+131	+132	+142	+141
	Δr(C1—H3) (Å)	+0.0011	+0.0008	+0.0005	+0.0005	+0.0003	+0.0005
	$\Delta\nu$(C1—H3) (cm^{-1})	−5, −8	−4, −6	−3, −3	−3, −3	−2, −3	−3, −3
	ΔE (kcal mol^{-1})	−6.48	−6.42	−4.58	−4.59	−4.43	−4.45
	ΔE^{CP} (kcal mol^{-1})	−3.84	−3.90	−4.18	−4.20	−4.09	−4.12
	$\Delta E^{CP,ZPE}$ (kcal mol^{-1})	−1.93	−2.28	−2.71	−2.79	−2.59	−2.67
B	r(O4· · ·H8) (Å)	2.1234	2.1682	2.1384	2.1616	2.1493	2.1729
	r(O10· · ·H5) (Å)	2.6164	2.8147	2.8268	2.8468	2.8528	2.8580
	Δr(N9—H8) (Å)	−0.0117	−0.0100	−0.0073	−0.0070	−0.0081	−0.0079
	$\Delta\nu$(N9—H8) (cm^{-1})	+178	+158	+129	+129	+139	+135
	Δr(C1—H5) (Å)	−0.0069	−0.0045	−0.0041	−0.0041	−0.0043	−0.0043
	$\Delta\nu$(C1—H5) (cm^{-1})	+85	+59	+55	+55	+55	+55
	ΔE (kcal mol^{-1})	−5.70	−5.56	−4.37	−4.38	−4.19	−4.21
	ΔE^{CP} (kcal mol^{-1})	−3.33	−3.44	−4.00	−4.02	−3.86	−3.89
	$\Delta E^{CP,ZPE}$ (kcal mol^{-1})	−1.70	−2.09	−2.70	−2.72	−2.56	−2.60

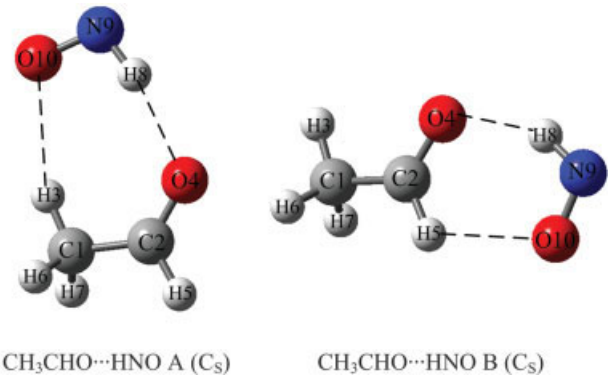

FIGURE 1. Optimized structure of complexes A and B.

sults are in good agreement with those of the B3LYP, which indicates that the N8—H9 and C2—H5 stretching frequencies exhibit large blue shift and the C1—H3 stretching frequency exhibits slight red shift in complexes A and B. To evaluate the influence of basis sets, the X—H stretching frequency changes were calculated by both MP2 and B3LYP methods with the 6-31G(*d*), 6-31+G(*d*,*p*) and 6-311++G(*d*,*p*) basis sets, respectively. Table I shows that the MP2/6-31+G(*d*,*p*) and MP2/6-311++G(*d*,*p*) values of the X—H stretching frequency change are in excellent agreement, while the corresponding MP2/6-31G(*d*) value is larger in magnitude. It appears that the larger the basis set is, the less the difference of the stretching frequency change. Influence of basis sets is also investigated for B3LYP calculation. Similar results are obtained. Taking the $(HF)_2$ complex as an example, Hobza and Halvaz [38] pointed out the necessity of using the CP-corrected gradient optimization. The CP-corrected gradient optimization will affect not only the interaction energy, but also the geometry and stretching frequency of the X—H···Y H-bond. However, the blue shift and red shift of the X—H stretching frequency in complexes A and B by both MP2 and B3LYP calculation is still in reasonable agreement with those of the X—H stretching frequency by standard optimization, as shown in Tables I and II, in spite of application of the CP-corrected optimization.

On the basis of these analyses, we can confirm that complex A simultaneously exhibits red-shifted C1—H3···O10 and blue-shifted N9—H8···O4 H-bonds. Complex B possesses simultaneously two blue-shifted H-bonds: N9—H8···O4 and C2—H5···O10. It should be pointed out that the N9—H8 stretching frequencies display very large blue shift (more than 100 cm^{-1}) in complexes A and B.

As shown in Tables I and II, the intermolecular interaction energies with both BSSE correction and ZPVE correction are in reasonable agreement at various levels. Furthermore, the results indicate that BSSE correction and ZPVE correction are important to accurately describe the intermolecular interaction energies. In addition, we note that complex B is slightly more stable than complex A.

AIM TOPOLOGICAL ANALYSIS

To confirm the existence of the H-bonds in complexes A and B, we performed AIM topological analysis. Popelier and colleagues [39, 40] proposed a set of criteria for the existence of H-bonds, among which three are most often applied [41]. The electron density and its Laplacian for the H···Y contact within the X—H···Y H-bond should have a relatively high value. Both parameters for closed-shell interactions as H-bond are positive and should be within the following ranges: 0.002–0.04 a.u. for the electron density and 0.02–0.15 a.u. for its Laplacian. According to the topological analysis of electron density in the theory of AIM, ρ is used to describe the strength of a bond. In general, the larger the value of ρ is, the stronger the bond is. The $\nabla^2\rho$ describes the characteristic of the bond. Where $\nabla^2\rho < 0$, the bond is covalent bond, as $\nabla^2\rho > 0$, the bond belongs to the ionic bond, hydrogen bond and van der Waals interaction. Here, $\nabla^2\rho = \lambda_1+\lambda_2+\lambda_3$, λ_i is an eigenvalue of the Hessian matrix of ρ. Then, when one of the three λ_i is positive and the other two are negative, we denote it by (3, −1) and call it the bond critical point (BCP). When one of the three λ_i is negative and the other two are positive, we denote it by (3, +1) and call it the ring critical point (RCP), which indicates that a ring structure exists. As shown in Table III, the values of the electron density ρ for O4···H8 and O10···H3 in complex A are 0.01701 and 0.00769 a.u., respectively. The values of the electron density ρ for O4···H8 and O10···H5 in complex B are 0.01731 and 0.00579 a.u., respectively. These values do fall within the proposed typical range of the H-bonds. Since the ρ(O4···H8) is larger than the ρ(O10···H3 or O10···H5) in complex A and B, we expect the former bond to be stronger than the latter. The values of the $\nabla^2\rho$ for O4···H8 and O10···H3 in complex A are 0.05115 and 0.02737 a.u., respectively. The values of the $\nabla^2\rho$ for O4···H8 and

TABLE III

Topological parameters of the bond critical point and ring critical point in complexes A and B at the MP2/6-31+G(*d,p*)

	BCP	ρ	$\nabla^2\rho$	λ_1	λ_2	λ_3
A	O4···H8	0.01701	0.05115	−0.02069	−0.01990	0.09174
	O10···H3	0.00769	0.02737	−0.00814	−0.00773	0.04324
B	O4···H8	0.01731	0.05161	−0.02147	−0.02027	0.09334
	O10···H5	0.00579	0.02378	−0.00543	−0.00510	0.03431
	RCP					
A	C1—C2—O4—H8—N9—O10—H3	0.00315	0.01689	−0.00239	0.00590	0.01338
B	C2—O4—H8—N9—O10—H5	0.00462	0.02527	−0.00356	0.00455	0.02428

O10···H5 in complex B are 0.05161 and 0.02378 a.u., respectively. These values are also in the range of the H-bonds. In addition, it is worthy of mentioning that there is a ring critical point (RCP) in complex A, which indicates that the seven-membered ring C1—C2—O4—H8—N9—O10—H3 exists in complex A. Similarly, The six-membered ring C2—O4—H8—N9—O10—H5 exists in complex B.

On the basis of the AIM topological analysis, we have proved that the N9—H8···O4, C1—H3···O10, and C2—H5···O10 can be classified as H-bonds in complexes A and B. It should be pointed out that the N9—H8 and C2—H5 bonds exhibit a large blue shift, whereas the C1—H3 bond exhibits a slight red shift. However, the AIM analysis does not reveal the origin of the red-shifted and blue-shifted H-bonds. This problem was solved by performing the natural bond orbital (NBO) analysis.

NBO ANALYSIS

It is clear from Figure 1 that the H-bonds are complicated in complexes A and B. Complex A exhibits simultaneously red-shifted C1—H3···O10 and blue-shifted N9—H8···O4 H-bonds. Complex B possesses two blue-shifted H-bonds. To interpret and explain the origins of the red-shifted and blue-shifted H-bonds in complexes A and B, we performed the NBO analysis and the corresponding results are presented in Table IV. In the NBO analysis, the importance of hyperconjugative interaction and electron density transfer (EDT) from lone electron pairs of the Y atom to the X—H antibonding orbital in the X—H···Y system is well-documented [35]. In general, such interaction leads to an increase in population of X—H antibonding orbital. The increase of electron density in X—H antibonding orbital weakens the X—H bond, which leads to its elongation and concomitant red shift of the X—H stretching frequency. Furthermore, Alabugin et al. [27] recently showed that structural reorganization of X—H bond in the process of both blue-shifted and red-shifted H-bonds was determined by the balance of the opposing effects: X—H bond lengthening effect due to hyperconjugative $n(Y) \rightarrow \sigma^*$ (X—H) interaction and X—H bond shortening effect due to rehybridization. On the basis of the theoretical model, it should not be difficult to explain the slight red shift of the C1—H3 stretching frequency in complexes A. For the C1—H3···O10 H-bond in complex A, Table IV shows that the hyperconjugative $n(O10) \rightarrow \sigma^*$ (C1—H3) interaction is relatively significant. The corresponding increase of electron density in the σ^* (C1—H3) weakens and elongates the C1—H3 bond, which results in the red shift of the C1—H3 stretching frequency. In contrast, according to the rehybridization model, the C1—H3···O10 H-bond formation increases C1—H3 bond polarization and positive charge on H3 atom. These changes result in a simultaneous increase in the *s*-character in the C1 hybrid orbital of C1—H3 bond, which should lead to C1—H3 bond contraction. Table IV shows that the *s*-character of the C1—H1 bond in the C1—H3···O10 H-bond increases from $sp^{2.88}$ to $sp^{2.79}$ which strengthens the C1—H3 bond. Because hyperconjugation and rehybridization act in opposite directions, the red shift and blue shift of the bond X—H is a result of a balance of the two effects. Then, the fact is

TABLE IV

NBO analysis of the HNO, CH_3CHO, and complexes A and B at the MP2/6-31+G(*d,p*) level.

	HNO	CH_3CHO	A	B
$E^{(2)}n_1$(O4) → σ^* (N9—H8) (kcal mol^{-1})	—	—	3.85	2.82
$E^{(2)}n_2$(O4) → σ^* (N9—H8) (kcal mol^{-1})	—	—	4.03	4.48
$E^{(2)}n_2$(O10) → σ^* (N9—H8) (kcal mol^{-1})	14.63	—	11.34	11.49
E-index (N9—H8· · ·O4)	—	—	0.42	0.43
σ^* (N9—H8)/*e*	0.02462	—	0.02838	0.02786
$\Delta\sigma^*$ (N9—H8)/*e*	—	—	0.00376	0.00324
n_2(O10)/*e*	1.96915	—	1.97442	1.97518
Δn_2(O10)/*e*	—	—	0.00527	0.00603
q(H8)/*e*	0.32756	—	0.36640	0.36513
spn(N9—H8)	$sp^{3.52}$	—	$sp^{3.02}$	$sp^{3.05}$
%*s*-char	22.10%	—	24.81%	24.63%
pol, N9%	67.23%	—	69.37%	69.29%
($\sigma_{N9—H8}$), H8%	32.77%	—	30.63%	30.71%
$E^{(2)}n_1$(O10) → σ^* (C1—H3) (kcal mol^{-1})	—	—	1.28	—
$E^{(2)}n_2$(O10) → σ^* (C1—H3) (kcal mol^{-1})	—	—	0.91	—
$E^{(2)}$ σ^* (C2—H5) → σ^* (C1—H3) (kcal mol^{-1})	—	3.05	2.87	—
E-index (C1—H3· · ·O10)	—	—	0.08	—
σ^* (C1—H3)/*e*	—	0.00580	0.00912	—
$\Delta\sigma^*$ (C1—H3)/*e*	—	—	0.00332	—
q(H3)/*e*	—	0.25323	0.27015	—
spn(C1—H3)	—	$sp^{2.88}$	$sp^{2.79}$	—
% *s*-char	—	25.73%	26.39%	—
pol, C1%	—	62.75%	63.72%	—
($\sigma_{C1—H3}$), H3%	—	37.25%	36.28%	—
$E^{(2)}n_1$(O10) → σ^* (C2—H5) (kcal mol^{-1})	—	—	—	0.49
$E^{(2)}n_2$(O10) → σ^* (C2—H5) (kcal mol^{-1})	—	—	—	0.21
$E^{(2)}n_1$(O4) → σ^* (C2—H5) (kcal mol^{-1})	—	1.44	—	2.62
$E^{(2)}n_2$(O4) → σ^* (C2—H5) (kcal mol^{-1})	—	26.54	—	22.85
E-index (C2—H5· · ·O10)	—	—	—	3.59
σ^* (C2—H5)/*e*	—	0.04646	—	0.04228
$\Delta\sigma^*$ (C2—H5)/*e*	—	—	—	−0.00388
q(H5)/*e*	—	0.14646	—	0.16822
spn(C2—H5)	—	$sp^{2.18}$	—	$sp^{2.13}$
% *s*-char	—	31.39%	—	31.92%
pol, C2%	—	58.53%	—	59.53%
($\sigma_{C2—H5}$), H5%	—	41.47%	—	40.47%

simple: the hyperconjugation is slightly dominant and overshadows the rehybridization in the C1—H3· · ·O10 H-bonds. To this point, the NBO results fully explain the observations of the slight red shift of the C1—H3 stretching frequency in complex A.

We pay more attention to the change of the C2—H5 stretching frequency in complex B. It is worth pointing out that the change of the C2—H5 stretching frequency in complex B has an evident difference from that of the C1—H3 stretching frequency in complex A. Although the hyperconjugative n(O10) → σ^* (C2—H5) interaction is relatively weak, the existence of relatively large blue shift of the C2—H5 stretching frequency is still surprising. This interaction should lead to the increase of electron density in the σ^* (C2—H5), which weakens the C2—H5 bond associated with its elongation. However, the opposite is found.

From Table IV, it can be seen that the electron density in the σ^* (C2—H5) decreased, which unambiguously means strengthening and contraction of the C2—H5 bond and blue shift of the stretching frequency. The question is how to explain the decrease of electron density in the σ^* (C2—H5). Hobza and colleagues [5, 6] showed that reason for

the decrease of electron density in σ^* (X—H) is electron density redistribution effect. On the basis of electron density redistribution effect, we will provide a reasonable model to explain the decrease of electron density in σ^* (X—H). In the type Z—X—H$\cdots$Y H-bond, where Z is an electronegative atom having one or more lone electron pairs (e.g., F, O, N), the hyperconjugative n(Y) $\rightarrow$ σ^* (X—H) interaction leads to an increase of electron density in the σ^* (X—H). In contrast, a decrease in the n(Z) $\rightarrow$ σ^* (X—H) interaction of complex, relative to the monomer, has the opposite effect. As a result, the net change of electron density in the σ^* (X—H) and the ultimate direction of the X—H bond length change depend on the balance of these two interactions, which changed in an antiparallel way. It may be of interest to make a quantitative comparison between these two interactions. Then, we define a novel index, called the *E*-index, which can be determined as a ratio of the variable magnitude of the n(Z) $\rightarrow$ σ^* (X—H) interaction and the magnitude of the n(Y) $\rightarrow$ σ^* (X—H) interaction in the Z—X—H$\cdots$Y system. Here, the *E*-index can be expressed as

$$E-\text{index}=\frac{E_{\text{monomer}}[n(\text{Z})\rightarrow\sigma^*(\text{X}-\text{H})]-E_{\text{complex}}[n(\text{Z})\rightarrow\sigma^*(\text{X—H})]}{E[n(\text{Y})\rightarrow\sigma^*(\text{X—H})]}, \quad (1)$$

where the $E_{\text{monomer}}[n(\text{Z}) \rightarrow \sigma^*$ (X—H)] and E_{complex} [n(Z) $\rightarrow$ σ^* (X—H)] mean the n(Z) $\rightarrow$ σ^* (X—H) interactions in the monomer and complex, respectively. The $E[n(\text{Y}) \rightarrow \sigma^*$ (X—H)] denotes the n(Y) $\rightarrow$ σ^* (X—H) interaction in the complex. According to the definition of the *E*-index, the *E*-index can be used to describe the strength of the electron density redistribution. In general, the larger the value of the *E*-index, the stronger the electron density redistribution effect. It can be seen in Table IV that there a significant decrease of the n_2(O4) $\rightarrow\sigma^*$ (C2—H5) in complex B, relative to the monomer CH_3CHO. Furthermore, the value of the *E*-index is very large and beyond 1.0, which indicates that the electron density redistribution effect is very significant in the C2—H5$\cdots$O10 H-bond of complex B. Consequently, the surprising phenomenon that the electron density in the σ^* (C2—H5) has an evident decrease can well be interpreted. In addition, according to the rehybridization model, the *s*-character of sp^n hybrid orbital for the C2—H5 bond increases from $sp^{2.18}$ to $sp^{2.13}$ upon the formation of the C2—H5$\cdots$O10 H-bond in complex B. On the basis of these analyses, we can conclude that there are two effects to decrease the C2—H5 bond length and obtain a blue shift of the C2—H5 stretching frequency. The first effect is connected with an evident decrease of electron density in the σ^* (C2—H5). The second effect is connected with the rehybridization of sp^n C2—H5 hybrid orbital.

The situation in complex B is different from complex A. The electron density redistribution is not important for C1—H3 bond in complex A. The dominant part of the electron density transfer from n(O10) is directed to the σ^* (C1—H3). The corresponding increase of electron density in the σ^* (C1—H3) causes weakening of the C1—H3 bond.

For the N9—H8$\cdots$O4 H-bonds in complexes A and B, The hyperconjugative n(O4) $\rightarrow$ σ^* (N9—H8) interaction is beyond the 5 kcal/mol threshold, which indicates that the hyperconjugation is very important. However, it is surprising that the very large blue shift of N9—H8 stretching frequency was in fact observed in Tables I and II. The question is how to explain so large a blue shift of the N9—H8 stretching frequency. First, we note that the electron density redistribution plays a significant role. As shown in Table IV, the magnitude of n(O10) $\rightarrow$ σ^* (N9—H8) interactions have an evident change in the monomer HNO and complexes A and B. The interactions are stronger in the monomer HNO than in complexes A and B. A decrease in n(O10) $\rightarrow$ σ^* (N9—H8) interaction leads to a decrease of electron density in the σ^* (N9—H8). The relatively lager values of the *E*-index indicate that the electron density redistribution effect is relatively significant in the N9—H8$\cdots$O4 H-bonds of complexes A and B. As a result, it can be seen that the net increase of electron density in the σ^* (N9—H8) is relatively small in complexes A and B. We suggest that the N9—H8 bond lengthening effect of hyperconjugation can be greatly inhibited due to existence of the electron density redistribution effect. In contrast, it is worth noting that the rehybridization effect is very strong for the N9—H8 bonds in complex A and B. Table IV shows that the *s*-character of the sp^n hybrid orbitals increases from $sp^{3.52}$ to $sp^{3.02}$ for N9—H8 in complex A and from $sp^{3.52}$ to $sp^{3.05}$ for N9—H8 in complex B, respectively. The very large increase of *s*-character results in the intense

contraction of the N8—H9 bonds in complexes A and B.

According to the above analyses, the surprising large blue shift of N8—H9 stretching frequency can well be explained. Because the N8—H9 bond lengthening effect of hyperconjugation is greatly inhibited, we can expect that the N8—H9 bond shortening effect of rehybridization is dominant and overcomes the N8—H9 bond lengthening effect of hyperconjugation.

It should be pointed out that the HNO, CHO, and CH3 groups in the CH_3CHO have a significant difference. The HNO and CHO groups contain the O atom. In summary, it seems reasonable for us to assume Z—X—H group containing Z atom (Z is an electronegative atom and possesses one or more lone electron pairs) is a necessary condition for the existence of the significant electron density redistribution. When the hyperconjugative interaction is relatively weak and electron density redistribution effect is significant in the Z—X—H···Y H-bond, we would expect electron density in the σ^* (X—H) has a decrease. When the hyperconjugation interaction is relatively strong and electron density redistribution effect is significant in the Z—X—H···Y H-bond, we believe that the hyperconjugation can be greatly inhibited.

Conclusions

Two stable complexes $CH_3CHO\cdots HNO$ have been investigated using both standard and counterpoise-corrected (CP) optimization at the MP2/6-31G(*d*), MP2/6-31+G(*d*,*p*), MP2/6-311++G(*d*,*p*), B3LYP/6-31G(*d*), B3LYP/6-31+G(*d*,*p*) and B3LYP/6-311++G(*d*,*p*) levels, respectively. Complex A exhibits simultaneously C1—H3···O10 red-shifted and N9—H8···O4 blue-shifted H-bonds. Complex B possesses simultaneously two blue-shifted H-bonds: C2—H5···O10 and N9—H8···O4. The calculations show that the N9—H8 stretching frequency displays a very large blue shift (more than 100 cm^{-1}) in complexes A and B. From the NBO analysis, it becomes evident that the C1—H3···O10 red-shifted H-bond can be explained on the basis of the fact that the bond lengthening effect of hyperconjugation overcomes the bond shortening effect of rehybridization. For the C2—H5···O10 blue-shifted H-bond, NBO analysis fully interprets the electron density decrease of the σ^* (C2—H5) due to existence of the significant electron density redistribution effect. We conclude that the blue shift of the C2—H5 stretching frequency is due to an intricate combination of two shortening effects of the electron density decrease in the σ^* (C2—H5) and the rehybridization of sp^n C2—H5 hybrid orbital. For the N9—H8···O4 blue-shifted H-bonds in complexes A and B, the N9—H8 bond lengthening effect of hyperconjugation is greatly inhibited due to existence of the electron density redistribution effect. Consequently, the N9—H8 bond shortening effect is dominant, which leads to a large blue shift of N9—H8 stretching frequency.

ACKNOWLEDGMENTS

The authors express our gratitude to the referees for their value comments.

References

1. Delanoye, S. N.; Herrebout, W. A.; van der Veken, B. J. J Am Chem Soc 2002, 124, 11854.
2. Hobza, P.; Špirko, V.; Havlas, Z.; Buchhold, K.; Reimann, B.; Barth, H.-D.; Brutschy, B. Chem Phys Lett 1999, 299, 180.
3. Reimann, B.; Buchhold, K.; Vaupel, S.; Brutschy, B.; Havlas, Z.; Špirko, V.; Hobza, P. J Phys Chem A 2001,105, 5560.
4. Hobza, P.; Špirko, V.; Selzle, H. L.; Schlag, E. W. J Phys Chem A 1998, 102, 2501.
5. Chocholoušová, J.; Špirko, V.; Hobza, P. Phys Chem Chem Phys 2004, 6, 37.
6. Hobza, P.; Špirko, V. Phys Chem Chem Phys 2003, 5, 1290.
7. Mrázková, E.; Hobza, P. J Phys Chem A 2003,107, 1032.
8. Hobza, P. Int J Quantum Chem. 2002, 90, 1071.
9. Hobza, P.; Havlas, Z. Chem Rev 2000, 100, 4253.
10. Karpfen, A.; Kryachko, E. S. J Phys Chem A 2003, 107, 9724.
11. Kryachko, E. S.; Zeegers-Huyskens, T. J Phys Chem A 2001, 105, 7118.
12. Kryachko, E. S.; Zeegers-Huyskens, T. J Phys Chem A 2003, 107, 7546.
13. McDowell, S. A. J Chem Phys 2003, 119, 3711.
14. McDowell, S. A. J Chem Phys 2003, 118, 7283.
15. McDowell, S. A. Phys Chem Chem Phys 2003, 5, 808.
16. McDowell, S. A. J Mol Struct (Theochem) 2003, 625, 243.
17. Matsuura, H.; Yoshida, H.; Hieda, M.; Yamannaka, S.; Harada, T.; Shin-ya, K.; Ohno, K. J. Am Chem Soc 2003, 125, 13910.
18. Yoshida, H.; Harada, T.; Murase, T.; Ohno, K.; Matsuura, H. J Phys Chem A 1997, 101, 1731.
19. Harada, T.; Yoshida, H.; Ohno, K.; Matsuura, H. Chem Phys Lett 2002, 362, 453.
20. Gu, Y.; Kar, T.; Scheiner, S. J Am Chem Soc 1999, 121, 9411.
21. Scheiner, S.; Grabowski, S. J.; Kar, T. J Phys Chem A 2001, 105, 10607.
22. Scheiner, S.; Kar, T. J Phys Chem A 2002, 106, 1784.

23. Fang, Y.; Fan, J. M.; Liu, L.; Li, X. S.; Guo, Q. X. Chem Lett 2002, 31, 116.
24. Li, X. S.; Liu, L.; Scheiner, H. B. J Am Chem Soc 2002, 124, 9636.
25. Hermansson, K. J Phys Chem A 2002, 106, 4695.
26. Masunov, A.; Dannenberg, J. J.; Contreras, R. J Phys Chem A 2001, 105, 4737.
27. Alabugin, I. V.; Manoharan, M.; Peabody, S.; Weinhold, F. J Am Chem Soc 2003, 125, 5973.
28. Alabugin, I. V.; Manoharan, M.; Weinhold, F. J Phys Chem A 2004, 108, 4270.
29. Lu, P.; Liu, G. Q.; Li, J. C. J Mol Struct (Theochem) 2005, 723, 95.
30. D'Anna, B.; Bakken, V.; Beukes, J. A.; Nielsen, C. J.; Brudnik, K.; Jodkowski, J. T. Phys Chem Chem Phys 2003, 5, 1790.
31. Bunte, S. W.; Rice, B. M.; Chabalowski, C. F. J Phys Chem A 1997, 101, 9430.
32. Jalbout, A. F.; Darwish, A. M.; Alkahby, H. Y. J Mol Struct (Theochem) 2002, 585, 199.
33. Simon, S.; Duran, M.; Dannenbery, J. J. J Chem Phys 1996, 105, 11024.
34. Boys, S. F.; Bernardi, F. Mol Phys 1970, 19, 553.
35. Reed, A. E.; Curtiss, L. A.; Weinhold, F. Chem Rev 1988, 88, 899.
36. Bader, R. F. W. Atoms in Molecules: A Quantum Theory. Oxford University Press: Oxford, 1990.
37. Frisch, M. J.; Trucks, G. W.; Schlegel, H. B.; Scuseria, G. E.; Robb, M. A.; Cheeseman, J. R.; Montgomery, J. A., Jr.; Vreven, T.; Kudin, K. N.; Burant, J. C.; Millam, J. M.; Iyengar, S. S.; Tomasi, J.; Barone, V.; Mennucci, B.; Cossi, M.; Scalmani, G.; Rega, N.; Petersson, G. A.; Nakatsuji, H.; Hada, M.; Ehara, M.; Toyota, K.; Fukuda, R.; Hasegawa, J.; Ishida, M.; Nakajima, T.; Honda, Y.; Kitao, O.; Nakai, H.; Klene, M.; Li, X.; Knox, J. E.; Hratchian, H. P.; Cross, J. B.; Adamo, C.; Jaramillo, J.; Gomperts, R.; Stratmann, R. E.; Yazyev, O.; Austin, A. J.; Cammi, R.; Pomelli, C.; Ochterski, J. W.; Ayala, P. Y.; Morokuma, K.; Voth, G. A.; Salvador, P.; Dannenberg, J. J.; Zakrzewski, V. G.; Dapprich, S.; Daniels, A. D.; Strain, M. C.; Farkas, O.; Malick, D. K.; Rabuck, A. D.; Raghavachari, K.; Foresman, J. B.; Ortiz, J. V.; Cui, Q.; Baboul, A. G.; Clifford, S.; Cioslowski, J.; Stefanov, B. B.; Liu, G.; Liashenko, A.; Piskorz, P.; Komaromi, I.; Martin, R. L.; Fox, D. J.; Keith, T.; Al-Laham, M. A.; Peng, C. Y.; Nanayakkara, A.; Challacombe, M.; Gill, P. M. W.; Johnson, B.; Chen, W.; Wong, M. W.; Gonzalez, C.; Pople, J. A. Gaussian 03; Revision B.02; Gaussian: Pittsburgh, PA, 2003.
38. Hobza, P.; Halvas, Z. Theor Chim Acta 1998, 99, 372.
39. Kock, U.; Popelier, P. L. A. J Phys Chem 1995, 99, 9747.
40. Popelier, P. L. A. J Phys Chem A. 1998, 102, 1873.
41. Lipkowski, P.; Grabowski, S. J.; Robinson, T. L.; Leszczynski, J. J Phys Chem A 2004, 108, 10865.